FEM-based stability charts for underground cavities in soft carbonate rocks: validation through case-study applications

Perrotti M.[1], Lollino P. [1], Fazio N.L. [1], Parise M. [1,2]

[1] CNR – IRPI, Bari, 70126, Italy
[2] Department of Earth and Geo-environmental Sciences, University of Bari "Aldo Moro", Bari, 70126 Italy

Abstract

The stability of man-made underground cavities in soft rocks interacting with overlying structures and infrastructures represents a challenging problem to be faced. Based upon the results of a large number of parametric two-dimensional (2D) finite-element analyses of ideal cases of underground cavities, accounting for the variability of cave geometrical features and rock mechanical properties, specific charts have been recently proposed in the literature to assess at a preliminary stage the stability of the cavities. The purpose of the present paper is to validate the efficacy of the stability charts by means of the application to several case studies of underground cavities, either subjected to collapse in the past or still stable. The stability charts proposed result to be performing to catch the stability conditions and, eventually, the conditions that lead to failure occurrence. For sinkholes already occurred, they show the importance of structural elements as pillars and internal walls in the stability of the whole quarry system, whereas, for cavities that have not reached failure, they can provide useful indications about the eventual proneness of the underground cavity to local or general instability phenomena.

1. Introduction

The presence of underground cavities as a result of past mining operations of soft rocks, to be used as building material, nowadays induce high risk conditions for those regions characterised by a large number of underground quarries and mines. In Apulia region (southern Italy), soft and very soft carbonate rocks as calcarenites of Pliocene or Pleistocene age, have been largely used (Parise 2010, 2012), especially in the last century, in many types of construction, so that a diffuse net of cavities, nowadays underlying urban areas and infrastructures, was excavated in the last century and abandoned afterwards. In recent years, several collapses affected some of these cavity systems, involving structures and roads located at the ground surface and, therefore, inducing high risk for human life and properties (Fiore and Parise 2013). These effects are caused by degradation processes of these rock materials as a consequence of weathering- or human-induced actions over time (Ciantia et al. 2015); as a consequence, the stability of the quarries may change after decades from the time of excavation, giving rise to local or global cave instabilities and failures.

The problem of assessing the stability of underground cavities in soft rocks is generally faced by means of approaches characterized by different levels of accuracy and reliability. Phenomenological and analytical approaches are generally chosen in the preliminary stage of the analysis to deduce if the rock mass is close to instability or not (Gesualdo et al. 2001; Fraldi and Guarracino 2009; Carter 2014). Later on, more deterministic and accurate approaches could be adopted, such as those based on numerical modelling (Goodings and Abdulla 2002; Ferrero et al. 2010; Parise and Lollino 2011; Castellanza et al. 2018). The latter approach can be very useful nowadays, because three-dimensional studies can be carried out due to the availability of powerful numerical codes, which are capable of treating a wide range of problems related to the structural features of the rock mass examined (for both continuous or discontinuous rock masses). However, although remaining the most efficient way to dealing with stability problems at the specific site scale, sophisticated numerical techniques cannot be applied effectively to a large dataset of stability assessments because they require a large amount of detailed input data, which are not frequently available, and consequently they cannot be practically used for a preliminary evaluation. On the contrary, wide regions throughout the world are characterized by a huge number of cavities affecting the underground environment, so that representative three-dimensional numerical analyses cannot be developed efficiently for all the case studies. Therefore, in such cases, physically- or mechanically-based stability charts can be useful to provide a preliminary assessment on the stability of the underground system, as a function of the geometrical and mechanical parameters (Evangelista et al. 2003; Federico and Screpanti 2003; Suchowerska et al. 2012). It is worthwhile remarking that these approaches should be considered only as a preliminary stage of the complete procedure to be followed for the stability assessment (Castellanza et al. 2018, Fiore et al. 2018). Therefore, when a medium to high level of hazard comes out from the application of the charts here proposed, more detailed and site-specific investigations must necessarily be applied.

2. FEM-based underground cave stability charts

Perrotti and co-authors (2018) have proposed a two-dimensional finite element parametric study that account for ideal schemes of rectangular cavities, as shown in Figure 1, with variable geometrical parameters, as the cavity width (L), the cavity height (h) and the overburden thickness (t). A large set of 2D finite-element analyses were carried out using Plaxis-2D software in order to evaluate possible correlations between geometrical features of cavities and material strength parameters. The ranges of variation of these variables are consistent with the typical intervals of values observed for man-made Apulian underground quarries excavated in soft carbonate rocks, belonging to the Calcarenite di Gravina formation (Coviello et al. 2005; Andriani and Walsh 2010; Ciantia et al. 2015). In particular, the width of cavity, L, is assumed to vary in a range from 1 to 30 meters, the height of cavity, h, in a range from 2 to 8 meters, and the overburden thickness, t, in a range from 2 to 10 meters. Additional 3D-FEM analyses were also performed to evaluate the effect of the rock confinement in the third direction, which, generally, results in increasing the stability of underground quarries with respect to the 2D analyses.

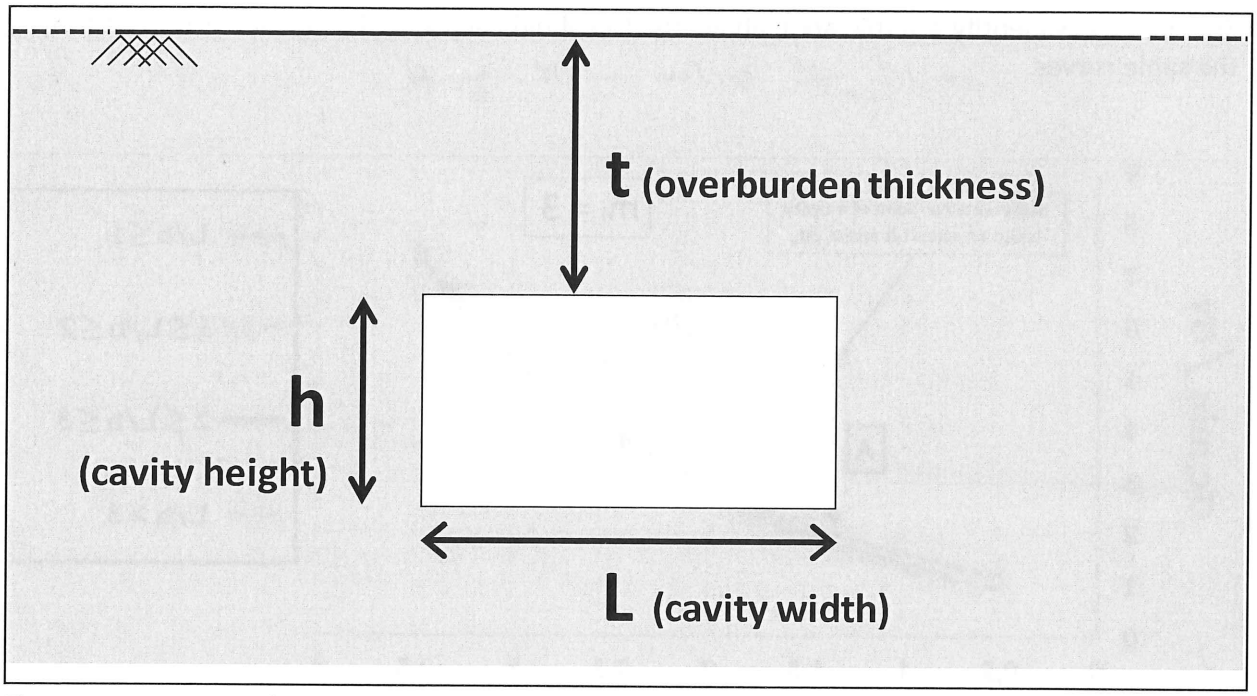

Figure 1. Geometrical parameters of the cavity (h = cavity height; L = cavity width; t = overburden thickness).

The mechanical behaviour of the soft and very soft carbonate rocks has been schematised according to an elastic perfectly plastic constitutive model characterized by a Hoek-Brown failure criterion (Hoek and Brown, 1997; Hoek and Martin, 2014), which is capable to simulate a nonlinear strength envelope in the Mohr's plane, as generally observed for calcarenite rocks; the main mechanical variable chosen in the parametric analyses was the threshold value of uniaxial compressive strength $\sigma_{c,min}$, which corresponds to the activation of a failure mechanism for the cavity. Based upon field survey observations, which indicated that these rocks are rarely jointed, the rock mass was assumed to be intact and not affected by discontinuities, and consequently a geological strength index GSI (Hoek 1994) value equal to 100 was used in the analyses. It follows that the results obtained from the analyses cannot be considered valid for those cases where the rock mass is characterized by single joints or joint sets, so that the rock mass behaviour has a certain degree of anisotropy that cannot be disregarded. The parameter D, representative of the disturbance factor induced by the excavation technique, was prescribed equal to zero to simulate a rock mass that has not been disturbed or affected by stress release processes due to the specific hand-excavation technique adopted ~~throughout the whole~~ everywhere region (generally, this was the hand-excavation technique with chisels and hammers, adopted in order to obtain large blocks of calcarenites to be used as building material). The parameter m_i was defined, in first approximation, in accordance with the suggestions proposed by Cai (2010), to represent the ratio between the uniaxial compressive and tensile strength of the rock: three different values, equal to 3, 8 and 16 have been chosen in accordance with the values proposed by Hoek (2007) for the specific rock type, as well as with the results of uniaxial compressive and tensile strength tests performed on samples belonging to different varieties of the Gravina Calcarenite Formation (Andriani and Walsh, 2010).

other values? of D

→ Please write the equation you are using next! and after define the parameters and the assumptions

The resulting plots showing the $\sigma_{c,min}/\sigma_v$ ratio (i.e. threshold value of uniaxial compressive strength mobilized at failure divided by vertical stress before excavation, acting at the depth of the cavity roof) as a function of the non-dimensional ratio L/t, keeping fixed the non-dimensional cavity shape ratio L/h, are shown in Figures 2, 3 and 4, as referred to values of m_i equal, respectively, to 3, 8 and

16. The curves identify a stable area, above the threshold curves, and an unstable area underlying the same curves. identify the sectors on the graph.

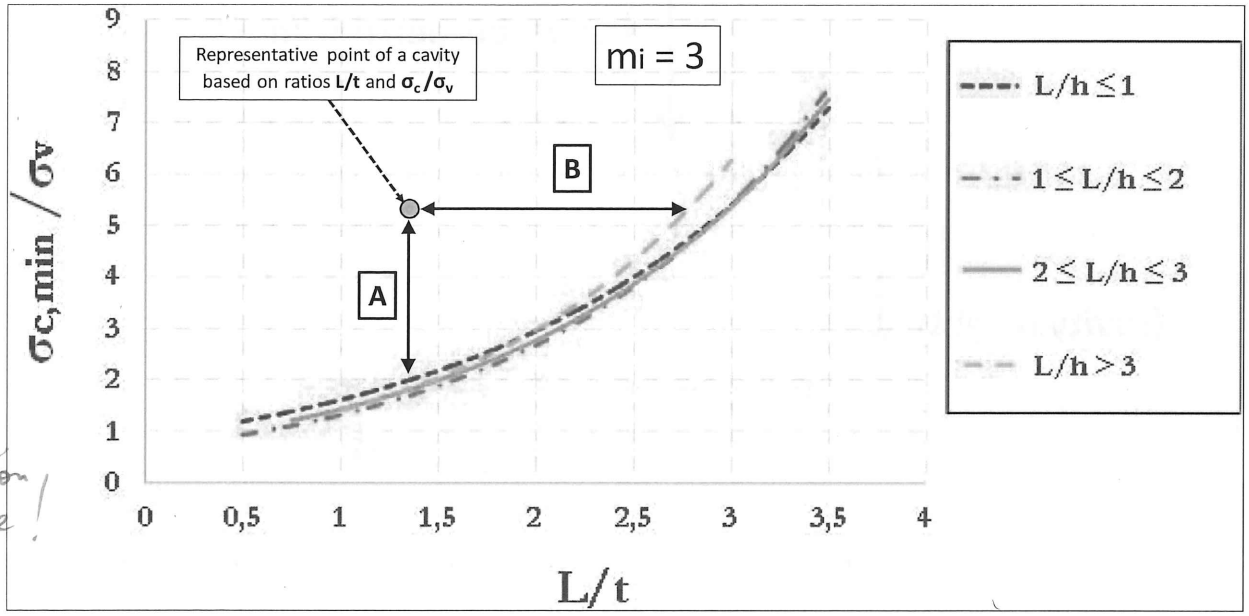

picture resolution or size!

Figure 2. Curves of $\sigma_{c,min}/\sigma_v$ against L/t for different values of the ratio L/h (mi = 3) (modified after Perrotti et al. 2018).

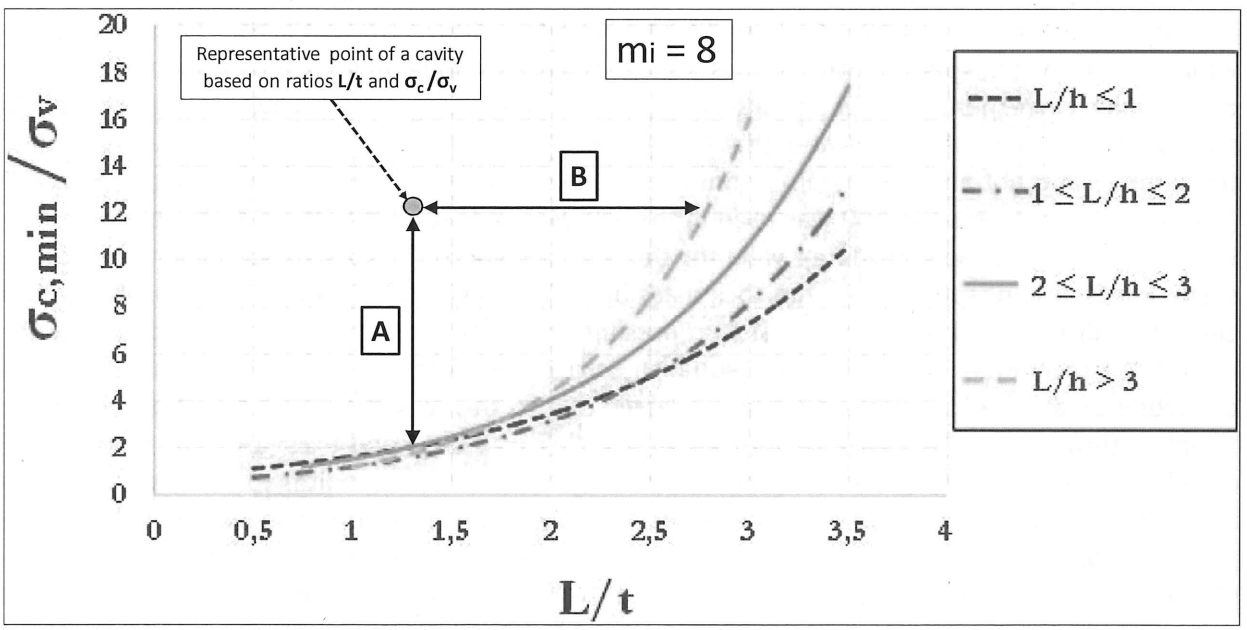

Figure 3. Curves of $\sigma_{c,min}/\sigma_v$ against L/t for different values of the ratio L/h (mi = 8) (modified after Perrotti et al. 2018).

And a 3rd zone = on the line!

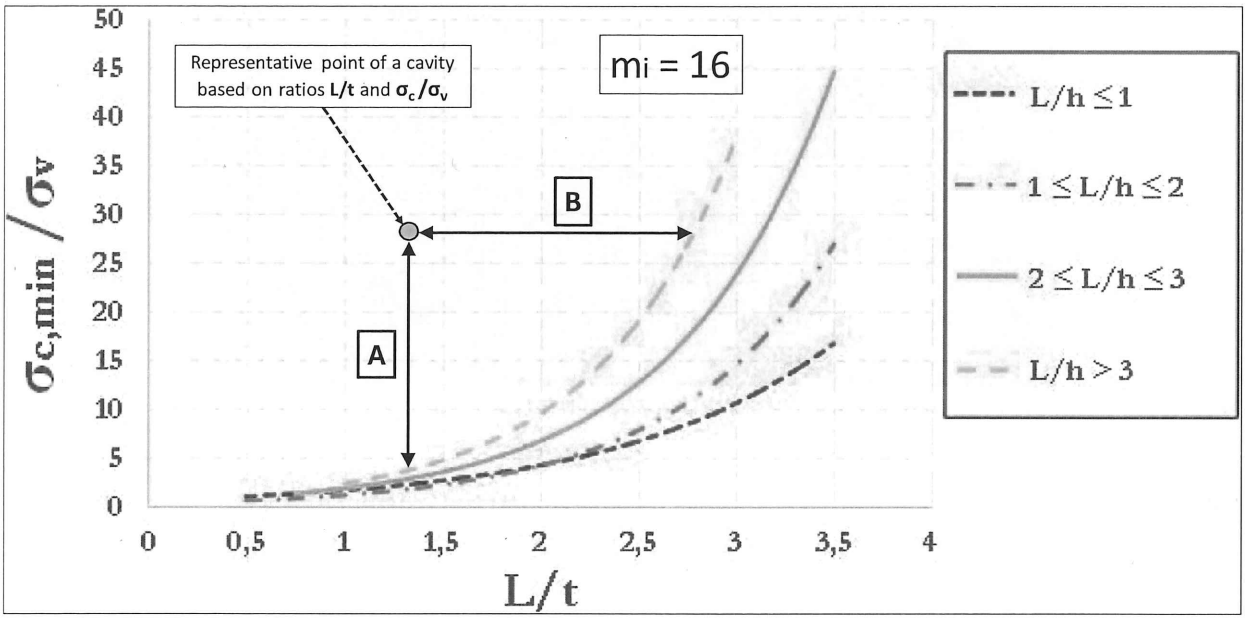

Figure 4. Curves of $\sigma_{c,min}/\sigma_v$ against L/t for different values of the ratio L/h (mi = 16) (modified after Perrotti et al. 2018).

These stability charts can be used to calculate the safety margin with respect to failure (segment A in Figure 2, 3 and 4) as the ratio between the actual in situ value of the rock uniaxial compressive strength (σ_c) and the threshold value for stability of the same parameter ($\sigma_{c,min}$) at the same L/t value. Alternatively, the same plots allow to calculate the maximum value of the width-to-depth ratio (L/t) allowed for stability (segment B), given the assigned value of the ratio between the in situ uniaxial compressive strength (σ_c) and the vertical stress (σ_v).

The following section describes some case studies of man-made underground cavities in soft calcarenites, either subjected to failure or stable, and the corresponding application of the FEM-based charts to evaluate the corresponding unstable or stable conditions as a function of the mechanical and geometrical parameters.

a bit hard to understand without equation

1. Remark: gather fig 2, 3, 4 in only one fig. and produce a second one to explain the meaning of A and B segments

2. What is the best fit(s) of a 3D FEM model? And How much?

3. How is the safety margin (or parameter) quantified? Which values selected to apply the graphs.

3. Application to case studies

Here: Nice to explain how and why these cases have been selected to apply the graphs: the main features of these one can be explained (already collapsed or not, mapped or unknown, ...) as in the conclusion

3.1. Barletta sinkhole

In the night between 2 and 3 May of 2010, a large sinkhole occurred in the rural area of "San Procopio" (De Giovanni et al. 2011; Parise et al. 2013), near the town of Barletta (Apulia, southern Italy); the maximum diameter of the depression has been calculated to be approximately equal to 32 m at the ground surface (Figure 5).

Figure 5. Aerial view of the sinkhole occurred in the Barletta area.

Later on, geological and speleological surveys have revealed the existence of a complex network of artificial tunnels excavated presumably between the 19th and the 20th century in order to extract calcarenite rocks as a building material (De Giovanni et al. 2011; Parise et al. 2013). These studies have revealed that the underground cavity was formed of wide and long tunnels with a large number of isolated pillars showing an irregular spatial distribution, as reported in Figure 6 . In the sinkhole area (N-W sector of the cavity), the spatial distribution of pillars was coarsen, as compared with the rest of the cavity system, and characterised by the presence of only 8 pillars located at a distance of about 10 ÷ 12 meters from the others; as such, these pillars were deemed to be heavily overloaded and probably subjected to high stress conditions.

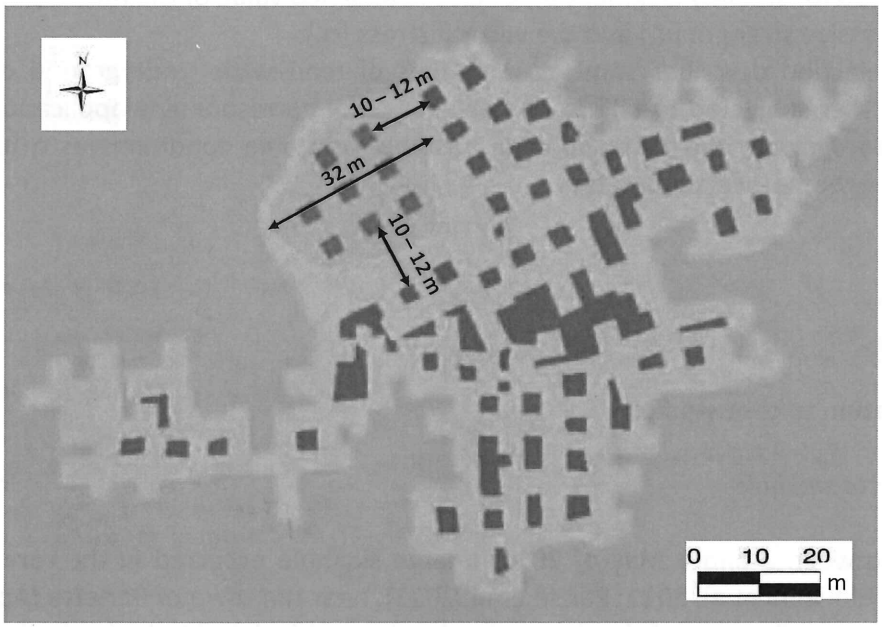

Figure 6. Schematic map of the Barletta underground calcarenite quarry (adapted after Luisi et al. 2015); the area involved in the collapse is shown in orange, pillars are in dark grey, and tunnels and excavated zones are in light grey.

184 Instability evidences, as signs of pillar crushing or fractures with detachments from the vault and
185 the walls (figure 7), were found throughout the cavity, especially close to the sinkhole area (De
186 Giovanni et al. 2011).

187

How are used the instability evidence?

Why do you show this?

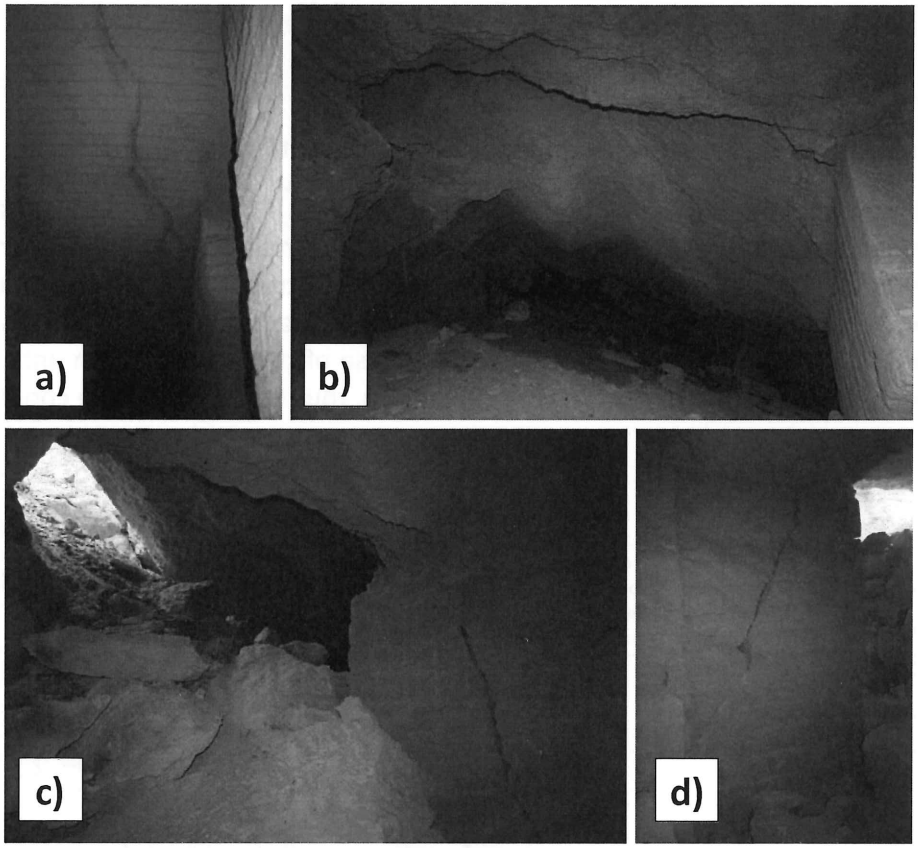

188

189 *Figure 7. Instability evidences at the Barletta underground quarry: a) tensile fracturing of the vault;*
190 *b) material detachment from the vault; c) open fractur on pillar, and vault collapses in the area*
191 *closest to the sinkhole rims; d) crushing of pillar with joints.* Source?

192

193 In order to verify the stability conditions using the charts proposed by Perrotti and co-authors
194 (2018), an initial value of the cavity width of about 10 ÷ 12 meters, corresponding to the largest
195 distance between two adjacent pillars (see Figure 6), has been assumed, bearing in mind that the
196 failure of the nearby pillars has presumably implied an increase of the effective L parameter.
197 Speleological surveys have indicated an average thickness of the calcarenite deposits in the study
198 area of about 6 m, with minimum value of 4 m (De Giovanni et al., 2011), with an upper layer of
199 about 0.5 ÷ 0.8 m composed of sandy-silty topsoil (unit weight γ = 20 kN/m^3) overlying a 5.2 ÷ 5.5
200 m thick calcarenite layer (unit weight γ = 17 kN/m^3. In the sinkhole area, the height of the cavity
201 rooms has been generally measured to be about 5 m.

202

203 Uniaxial compression tests performed in the laboratory on calcarenite samples taken in the sinkhole
204 area have indicated values of uniaxial compressive strength of about 1 ÷ 2 MPa under dry conditions
205 and about 0,75 ÷ 1 MPa under saturated conditions (Luisi et al. 2015); tensile strength values derived
206 from indirect tension tests have instead resulted to be approximately equal to 0.1 ÷ 0.2 MPa.

Remark: For this case and the next ones, please use a standard table with all the parameters and the values. Of course, keep the explanations related to the origin of these values (lab, tests, ...)

Consequently, the parameter m_i to be used in the Hoek & Brown failure criterion results in a range between 6 e 11.

Hence, based on these evaluations, the non-dimensional ratios L/t and L/h can be estimated in the following ranges: 1.66 < L/t < 2 and 2 < L/h < 2.4.

The vertical stress at a depth of h=6m is estimated to be equal to:

$\sigma_v \approx (\gamma_{calc} \cdot t_{calc}) + (\gamma_{topsoil} \cdot t_{topsoil}) = 104.4$ kPa

and, assuming $\sigma_c = 1$ MPa, a ratio σ_c/σ_v equal to about 9.6 is obtained.

Therefore, considering the chart corresponding to a value $m_i = 8$ (Figure 3), and specifically the curve corresponding to L/h ratio between 2 and 3, in the initial conditions (unfailed pillars) the cavity results to be in the stability zone (Figure 8); however, if a strength loss of the nearby pillars is accounted for, an increase of the L representative parameter leads to a gradual increase of the ratio L/t (as well as of L/h ratio), with the consequent decrease of the safety margin until reaching the threshold curve corresponding to the L/h value (Figure 8), thus indicating failure conditions.

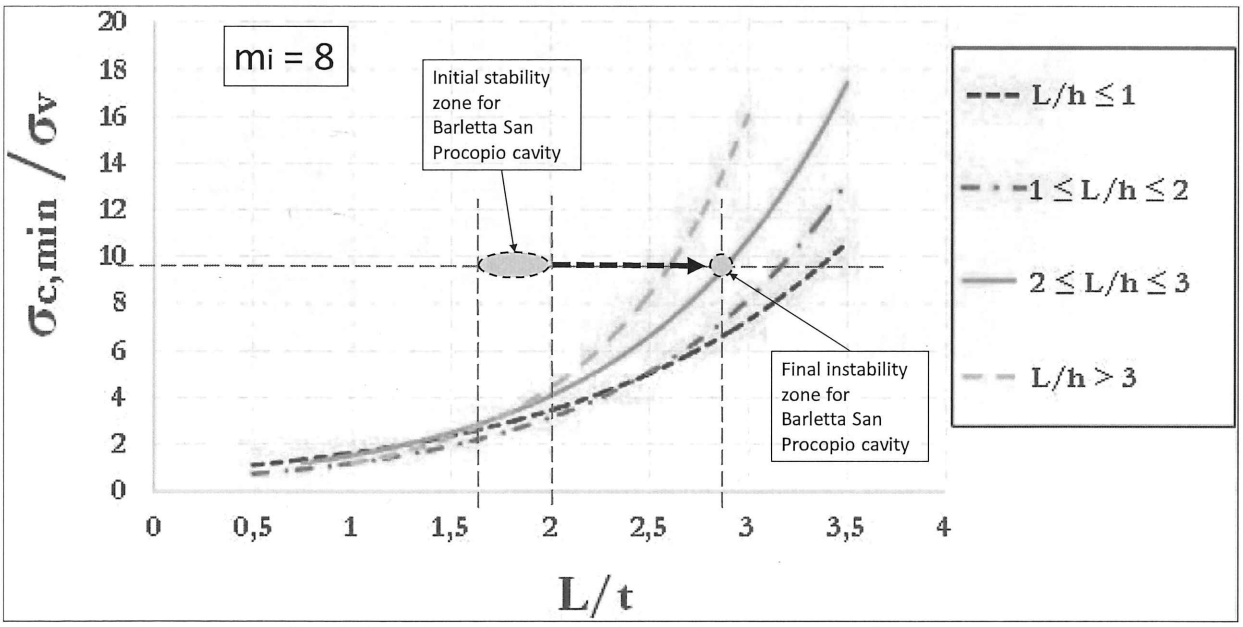

Figure 8. Application of stability chart (m_i=8) for the Barletta case study.

Figure 8 also shows that the cavity is close to failure conditions, already for values of ratio L/t larger than 2.5; therefore, even with the loss of the strength provided by a single pillar, a ratio L/t corresponding to the achievement of the threshold stability conditions follows.

3.2. Marsala sinkhole

A sinkhole took place in the town of Marsala (Sicily, Italy) in June 2011 in the area where underground quarries were excavated according to the room-and-pillar technique at depths ranging

from 3 ÷ 4 meters to about 15 m; after the quarry abandonment, since the 1960's, the cavity has been progressively subjected to instability phenomena, represented by deformations and block detachments from the vaults and the pillars.

A detailed map of the underground cavity luckily existed before the collapse, thanks to speleological survey carried out in 2000 (Vattano et al. 2013). This allowed to properly map the sinkhole boundary above the underground quarry; with a minimum diameter of about 25 ÷ 30 m at the ground level, the sinkhole is shown in Figure 9. The figure shows that the examined quarry consists of rooms with quadrangular shape, in most cases connected and/or separated by thin rock walls or pillars. As specifically concerns the sinkhole area, the excavation was carried out according to an irregular scheme, leaving very small pillars and slight internal walls; larger sizes of the internal supporting elements, as well as lower room spans, are instead observed in the rest of the cavity system. The average room height has been estimated to be equal to 2.7 m, with the roof thickness varying from 8.2 to 11.8 m.

Try to keep a similar way to present all the study cases!

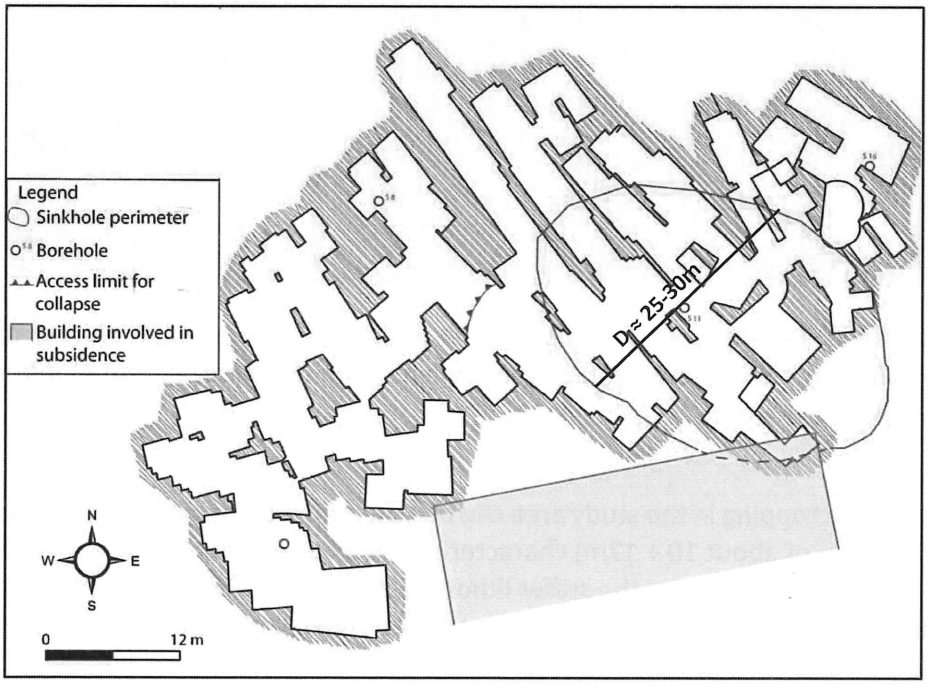

Figure 9. Plan of the Marsala underground quarry, with indication of the sinkhole area (adapted after Vattano et al. 2013).

For this study, Fazio et al. (2017) have proposed a three-dimensional Finite Element back-analysis and have found that the weakness of these overstressed internal structural elements could have been the reason for initial local failure, and then for global failure. In particular, the collapse of the pillars and the internal walls could have progressively entailed an increase in the width of the open galleries, leading to a total length, L, approximately equal to that of the sinkhole (D ≈ 25 ÷ 30m, Figure 9). Local failures of pillars and thin walls, as well as detachments and fracturing processes of the vault, are widely diffuse within the Marsala cavity, as documented in Figure 10.

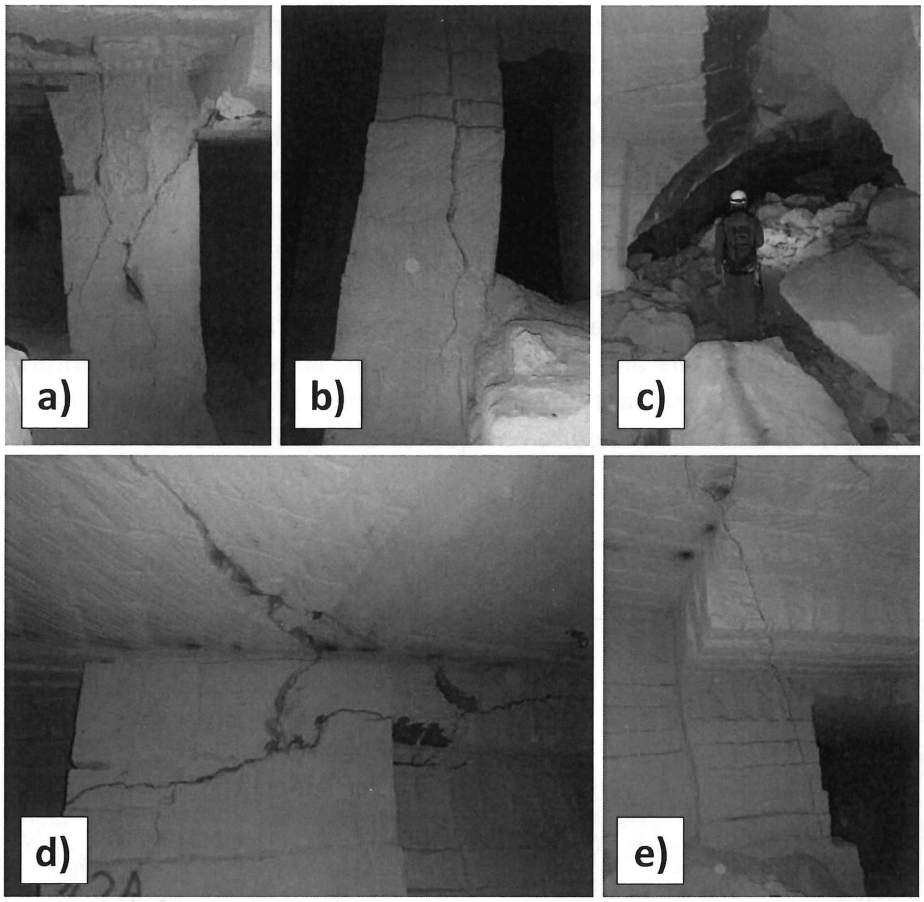

Figure 10. Instability evidences at the Marsala underground quarry: a) fracturing of a pillar; b) bending and failure of a pillar; c) material detachments from the vault; d) and e) diffuse fracturing within the walls and the vaults.

The calcarenites outcropping in the study area can be schematised according to two lithotypes, with a top layer (thickness of about 10 ÷ 12m) characterised by poor mechanical properties, and a stiffer deeper layer (Fazio et al. 2017). For the stiffer lithotype the dry unit weight is measured in the range between 12 and 15 kN/m^3, whereas the same parameter under saturated condition is between 13.5 and 17 kN/m^3. Uniaxial compressive strength under saturated conditions has been measured to reach about σ_c = 1.3 ÷ 1.6 MPa, whereas, with a saturation degree equal to zero, σ_c = 2 ÷ 3 MPa. The value of the tensile strength can be assumed to be 1/8 ÷ 1/10 of the compressive strength, in accordance with experimental works on similar calcarenite rocks (Andriani and Walsh 2010; Ciantia et al. 2015b), so that the m_i parameter to be used in the Hoek & Brown strength criterion results to be in a range between 8 e 10.

Based on the aforementioned parameters, considering a cavity width L ≈ 25 ÷ 30 m (corresponding to the collapse of internal pillars and walls in Figure 9), an average height h of 2.7 m and an average overburden thickness, t, of 10 m, the corresponding non-dimensional ratios L/t and L/h result to be in the following ranges: 2.5 < L/t < 3 and 9.2 < L/h < 11.1.

If a unit weight value γ_{calc} of 16 kN/m^3 is assumed, the vertical stress at depth of h = 10 m is equal to: $\sigma_v \approx (\gamma_{calc} \cdot t_{calc})$ = 160 kPa. Finally, assuming σ_c = 2 MPa (corresponding to an intermediate value between saturated and dry conditions), a ratio σ_c/σ_v approximately equal to 12.5 is obtained.

Figure 11 shows the representative state of the Marsala cavity stability in the stability chart corresponding to $m_i = 8$. The figure indicates that the state is located on the curve characterized by $L/h > 3$ and this confirms the unstable condition of the underground quarry.

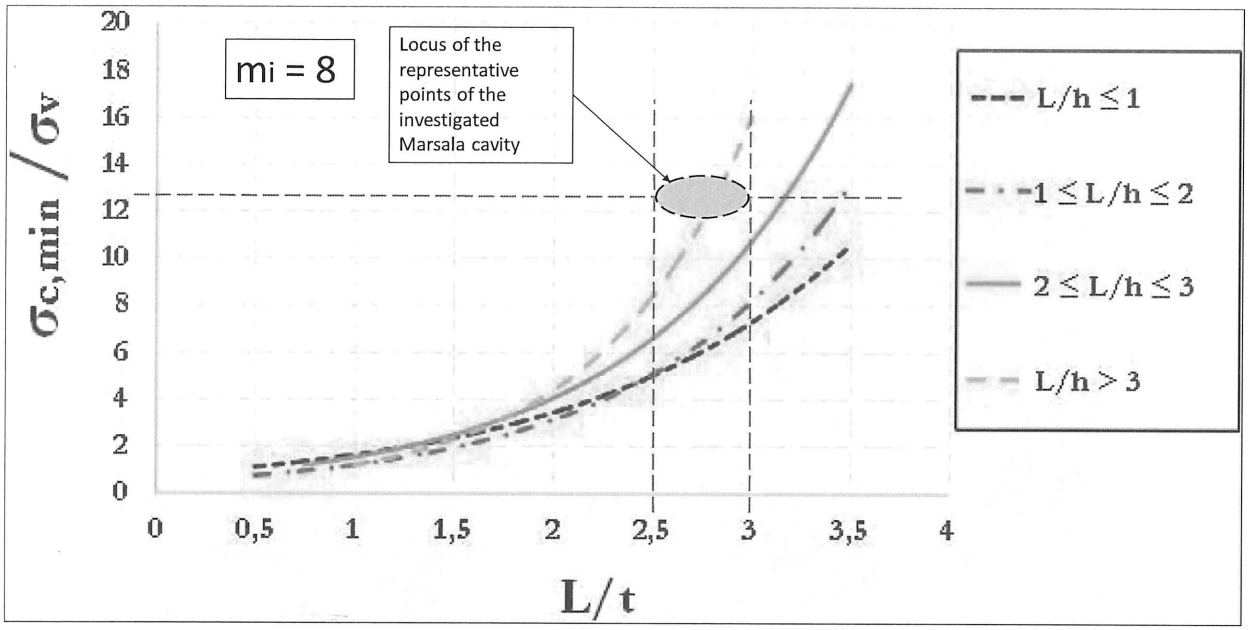

Figure 11. Application of stability chart ($m_i = 8$) for the Marsala underground quarry.

3.3. Gallipoli sinkhole

In the eastern urban area of the town of Gallipoli (southern Apulia) a large sinkhole occurred in 2007, between 29th March and 1st April, with the opening of a sub elliptical 12 m x 18 m chasm (Figure 12a), followed by a significant widening of the subsidence area at the ground level (Figure 12b) which affected some buildings located nearby.

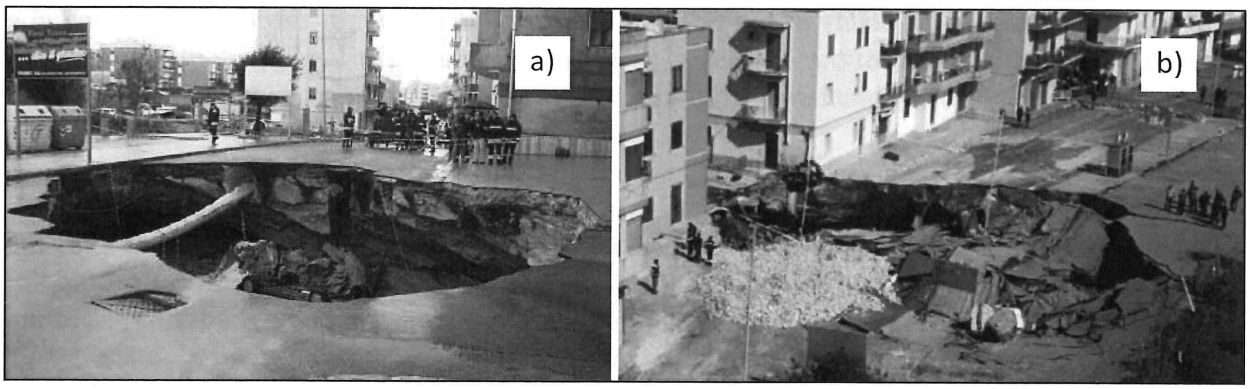

Figure 12. Pictures of the 2007 Gallipoli sinkhole: a) the first sinkhole as appeared in 29th March; b) enlargement of the chasm on 1st April. Source 7

306 Geological surveys performed soon after the collapse detected the existence of a complex
307 underground cavity net, on a single level; although a room-and-pillar excavation technique was
308 adopted, the resulting geometry of the cavity system is highly irregular, with rooms located at
309 variable depth from the ground level: in particular, in the area where sinkhole occurred, the depth
310 of the cave bottom is of about 8 m, with a roof thickness of less than 3 ÷ 4 meters. Moreover, diffuse
311 signs of local instability, as block detachments from the vault and the lateral walls, debris heaps on
312 the floor and fractures of pillars due to crushing were found within the cavity rooms (Delle Rose
313 2007; Parise 2012). Some of these local instabilities are shown in Figure 13.
314
315

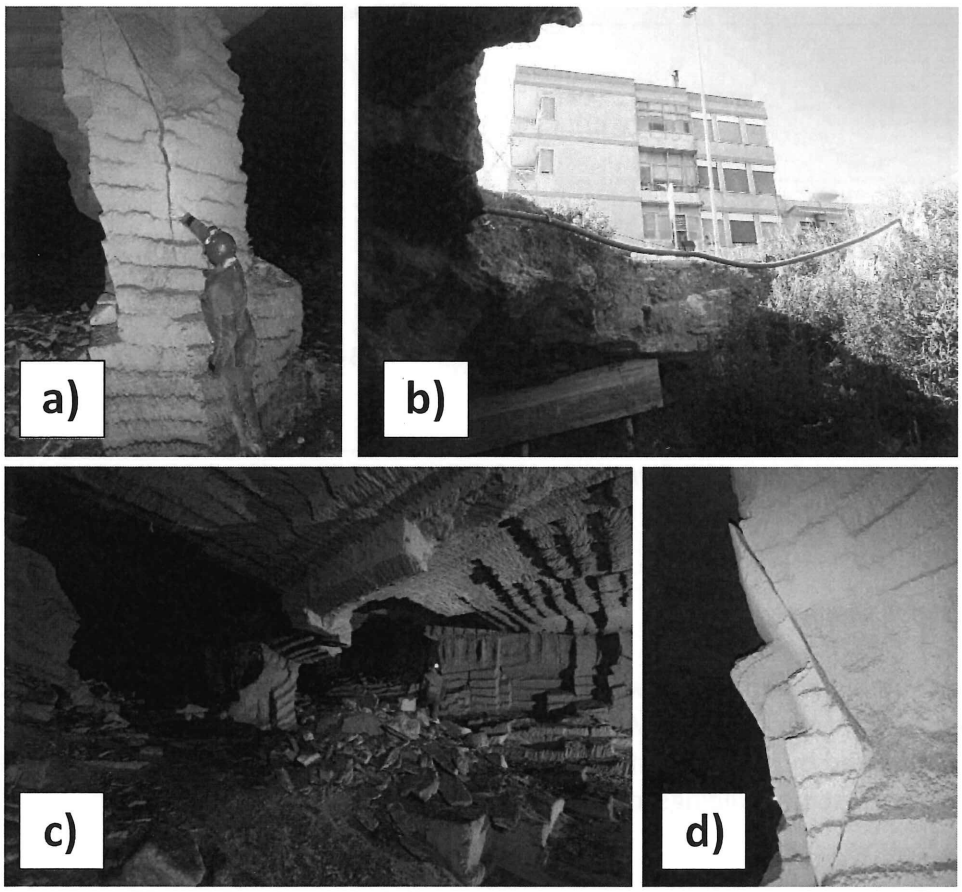

316
317 *Figure 13. Evidences of instability at the Gallipoli underground quarry: a) extensive fracturing in a*
318 *pillar; b) view of sinkhole from the bottom; c) inner view of one of the longest rooms in the cavity*
319 *(block detachments from the vault and debris heaps on the floor); d) incipient block detachment from*
320 *a pillar.*
321
322 Based on the investigations performed, a reconstruction of the cavity geometry, before the collapse,
323 has been carried out. Figure 14 shows the position of the remaining pillars, the zones with the
324 accumulation of debris or detachments of blocks and the detailed perimeter of the sinkhole, for
325 both the first collapse and the subsequent enlargement. The buildings and the roads on the ground
326 surface overlying the area are also shown in the map.
327
328

Why a so big picture? Please focus on the area of interest!

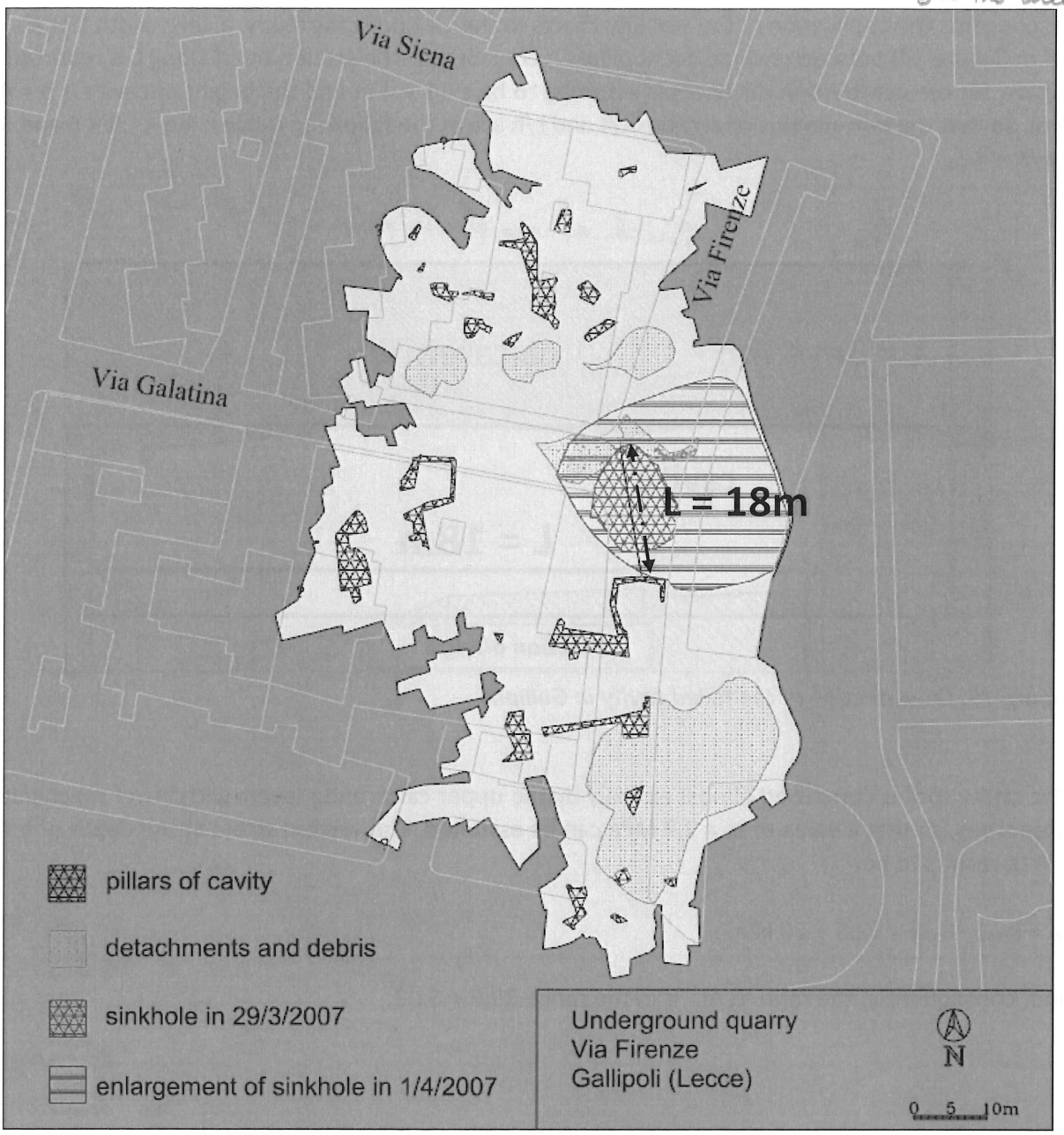

Figure 14. Map of the underground quarry in Via Firenze, Gallipoli, and overlying built environment.

Source?

In the sinkhole area, deposits of the Salento Calcarenites, consisting of alternations of calcarenite rocks and looser sediments, crop out; the rock volumes affected by the mining activity (i.e., the calcarenite) appear to be massive, whereas the upper layer, forming the cavity roof, is formed of laminated and stratified calcarenite deposits with very low mechanical properties (Delle Rose 2007; Parise 2012). Based on the saturation degree, uniaxial compressive strength σ_c results in a range between 2.5 and 3 MPa for dry samples and 1.7 ÷ 2.3 MPa for saturated rock (Ciantia et al. 2015). Tensile strength is variable between 0.7 and 1 MPa, so that a parameter $m_i = 3 \div 4$ of the Hoek & Brown failure criterion has been derived accordingly. A unit weight about equal to 17.5 kN/m^3 has been also assumed.

↳ in both dry and saturated states?

As concerns the application of the stability charts to the Gallipoli case study, a cave width L of about 18 m (Figure 14) between two adjacent pillars is considered. The section trace along L is reported in Figure 15; the overburden thickness is assumed to be t = 3 ÷ 4 m and the height of cavity is h = 4 ÷ 5 m, so that the non-dimensional ratios L/t and L/h are in the following ranges: 4.5 < L/t < 6 and 3.6 < L/h < 4.5.

Perfect! Such a graph is missing for the other cases.

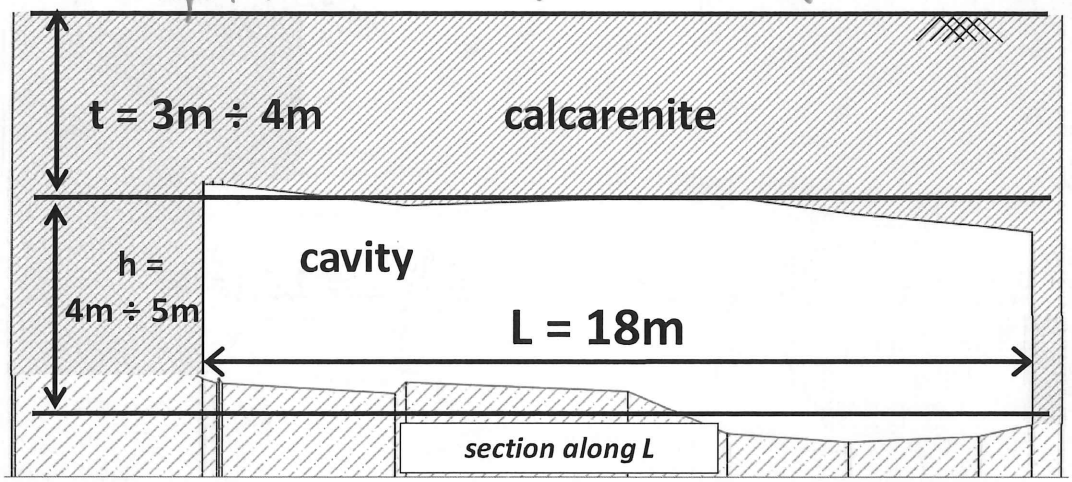

Figure 15. Cross-section of the failed cavity in Gallipoli.

The cavity roof is composed almost entirely by the upper calcarenite layers with lower mechanical properties, so that a value of σ_c = 2.7 MPa can be assumed. The vertical stress at the depth of h = 3 ÷ 4 m results to be:

$\sigma_v \approx (\gamma_{calc} \cdot t_{calc})$ = 52.5 ÷ 70 kPa;

and, consequently, the ratio σ_c/σ_v is in the range 38.6 ÷ 51.3.

use a tab with both min/max value to keep the implication of the σ_v range on the $\frac{\sigma_c}{\sigma_v}$ ratio variation

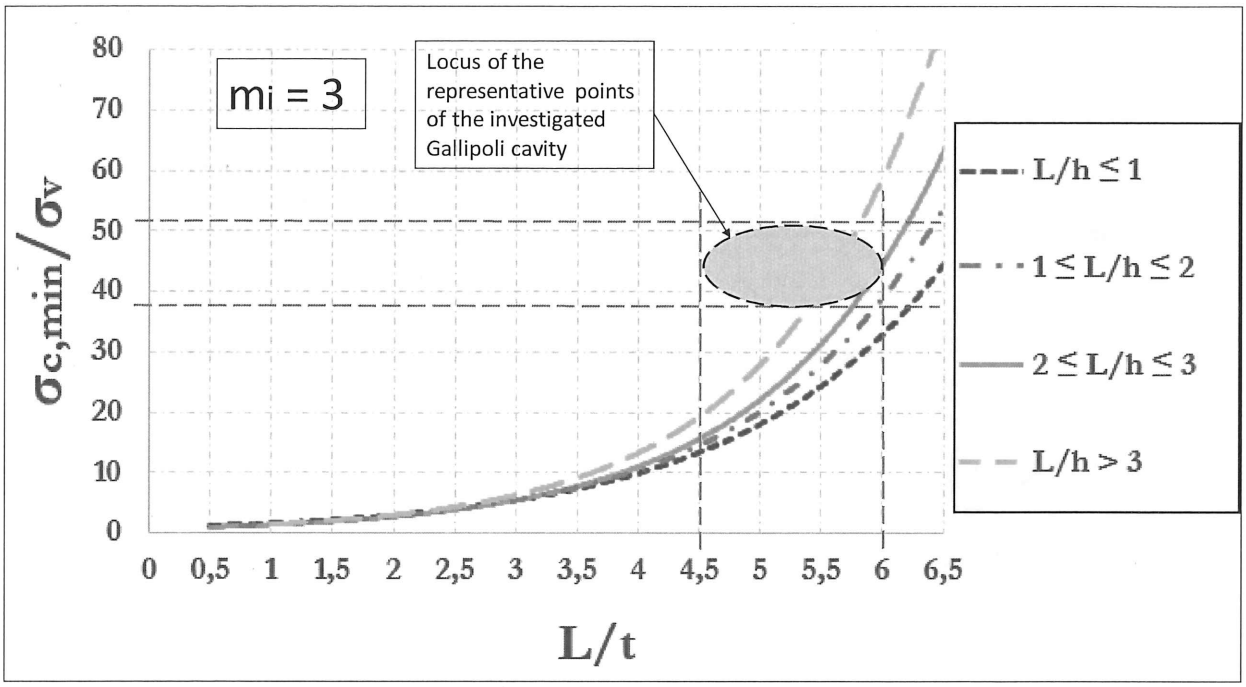

Figure 16. Application of stability chart (m_i = 3) for the Gallipoli underground quarry.

Taking into account the stability charts corresponding to m_i = 3 and, specifically, the threshold curve for L/h > 3, the representative area of the investigated cavity is very close to the threshold curve (Figure 16); therefore, it comes out that the cavity was in a state of incipient failure, so that some external factor, as for example vibrations or concentrated seepages, could have triggered the instability.

→ pipes or sewer leakages?

3.4. Cutrofiano underground caves

In the last century several underground quarries were excavated at the outskirts of the town of Cutrofiano (southern Apulia) with the room-and-pillar technique. Later on, these quarries were abandoned, and the urban area expanded above the areas originally interested by their development. Geological surveys have highlighted, in the southern part of the town, the existence of a diffuse net of underground cavities. The location of three quarries, respectively named as cave A, cave B and cave C, with respect to the overlying built-up environment, is reported in Figure 17.

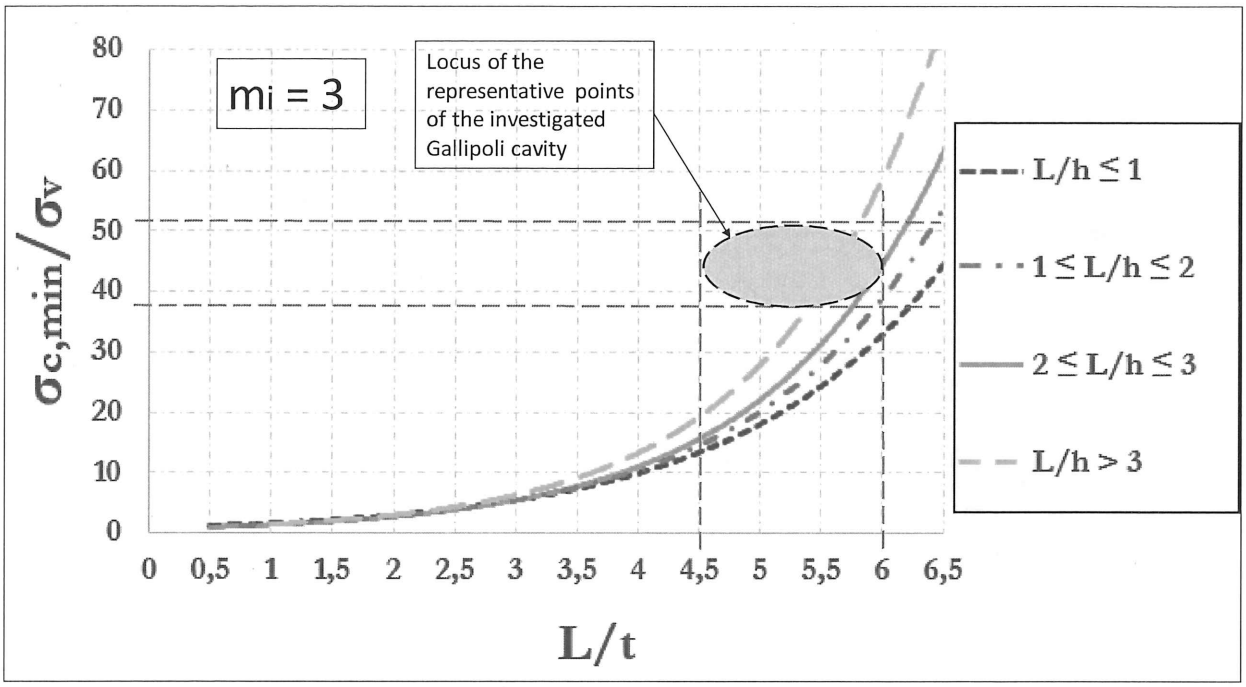

Figure 16. Application of stability chart (m_i = 3) for the Gallipoli underground quarry.

Taking into account the stability charts corresponding to m_i = 3 and, specifically, the threshold curve for L/h > 3, the representative area of the investigated cavity is very close to the threshold curve (Figure 16); therefore, it comes out that the cavity was in a state of incipient failure, so that some external factor, as for example vibrations or concentrated seepages, could have triggered the instability.

→ pipes or sewer leakages?

3.4. Cutrofiano underground caves

In the last century several underground quarries were excavated at the outskirts of the town of Cutrofiano (southern Apulia) with the room-and-pillar technique. Later on, these quarries were abandoned, and the urban area expanded above the areas originally interested by their development. Geological surveys have highlighted, in the southern part of the town, the existence of a diffuse net of underground cavities. The location of three quarries, respectively named as cave A, cave B and cave C, with respect to the overlying built-up environment, is reported in Figure 17.

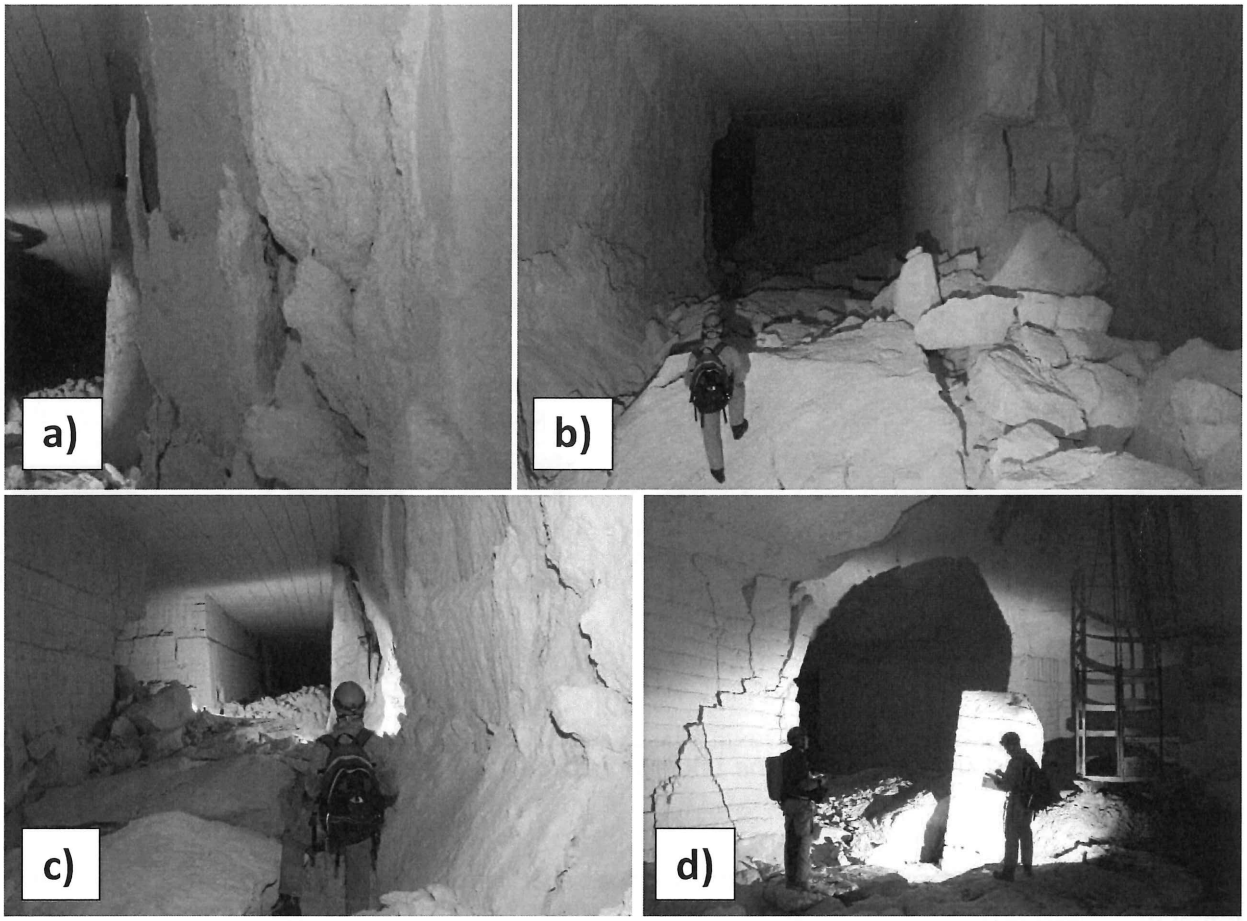

Figure 18. Signs of local instability in the Cutrofiano underground quarries: a) diffuse fracturing of a wall; b) detachments of material from walls; c) massive falls from the walls, with heavy production of debris heaps on the floor; d) open fractures at the pillars rim, in correspondence of the main shaft of access to the cavity.

For each of the examined cavities, a detailed geometrical and geological survey has been performed. The geological setup of the area is formed of shallow layers of clays, silts and/or sands that overlie a stiffer layer of calcarenite, locally named "Mazzaro", which generally represent the roof of the quarries. Therefore, in order to apply the stability charts the "Mazzaro" level has been considered. From a geomechanical point of view, unit weight values in the range of 18.6 ÷ 19.6 kN/m^3 for sandy layers and 19.8 ÷ 20.5 kN/m^3 for the calcarenite layer has been respectively accounted for. A uniaxial compressive strength of about 2.4 MPa has been measured for the Mazzaro material forming the cave roofs (Lollino & Parise 2010), whereas the tensile strength is about 1/10 of the compressive one, so that the parameter m_i of the Hoek & Brown failure criterion is assumed to be equal to m_i = 8. In the following sub-sections, the representative conditions of each cavity are shown with respect to the corresponding chart.

3.4.1. Cave A

The stability analysis for cavity A has been carried out with reference to the cross-section AA in Figure 19. The width and height of cavity, are, respectively, equal to L = 7.50 m and h = 5.0 m, while the thickness of the resistant portion of the cave roof, which in this case is coincident with the

"Mazzaro" rocky layer, is t = 4.30 m. Therefore, the non-dimensional ratios result to be about L/t ≈ 1.74 and L/h ≈ 1.5.

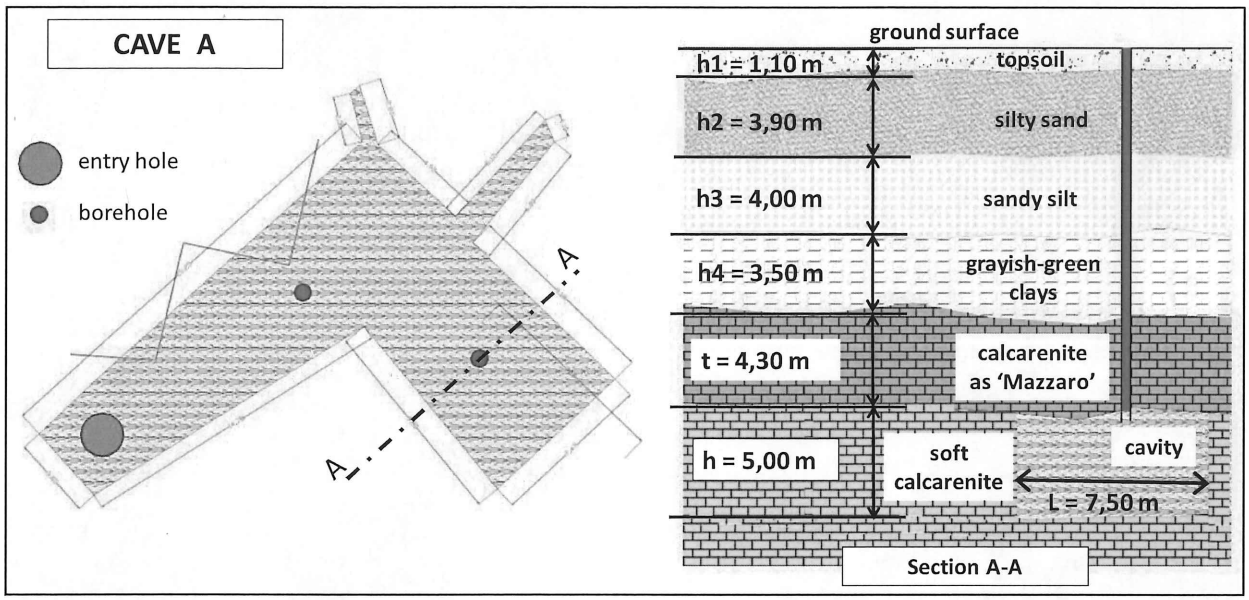

Figure 19. Plan and stratigraphy of the underground cavity A (adapted from Maglio and Ligori, 2014).

With reference to the stratigraphy in Figure 15, the vertical stress at the depth of the cavity roof is equal to:

$$\sigma_v \approx (\gamma_1 \cdot t_1) + (\gamma_2 \cdot t_2) + (\gamma_3 \cdot t_3) + (\gamma_4 \cdot t_4) + (\gamma_{mazzaro} \cdot t_{mazzaro}) = 324.62 \text{ kPa}$$

so that, if $\sigma_{c,min}$ = 2.4 MPa, we obtain an operative value of $\sigma_c/\sigma_v \approx 7.39$.

3.4.2. Cave B

For cave B the calculation has been performed for section B-B in Figure 20. It has to be noted that in this case a two story civil building exists just above the cavity, thus representing a further overburden stress, which has been approximately evaluated equal to q = 100 kPa.
The width and the height of the cavity are equal to L = 6.80 m and h = 5.00 m, respectively, while the thickness of the resistant beam-shaped portion of the roof, i.e. the "Mazzaro" layer, is t = 2.70 m. Therefore, the non-dimensional ratios result to be about L/t ≈ 2.52 and L/h ≈ 1.36.

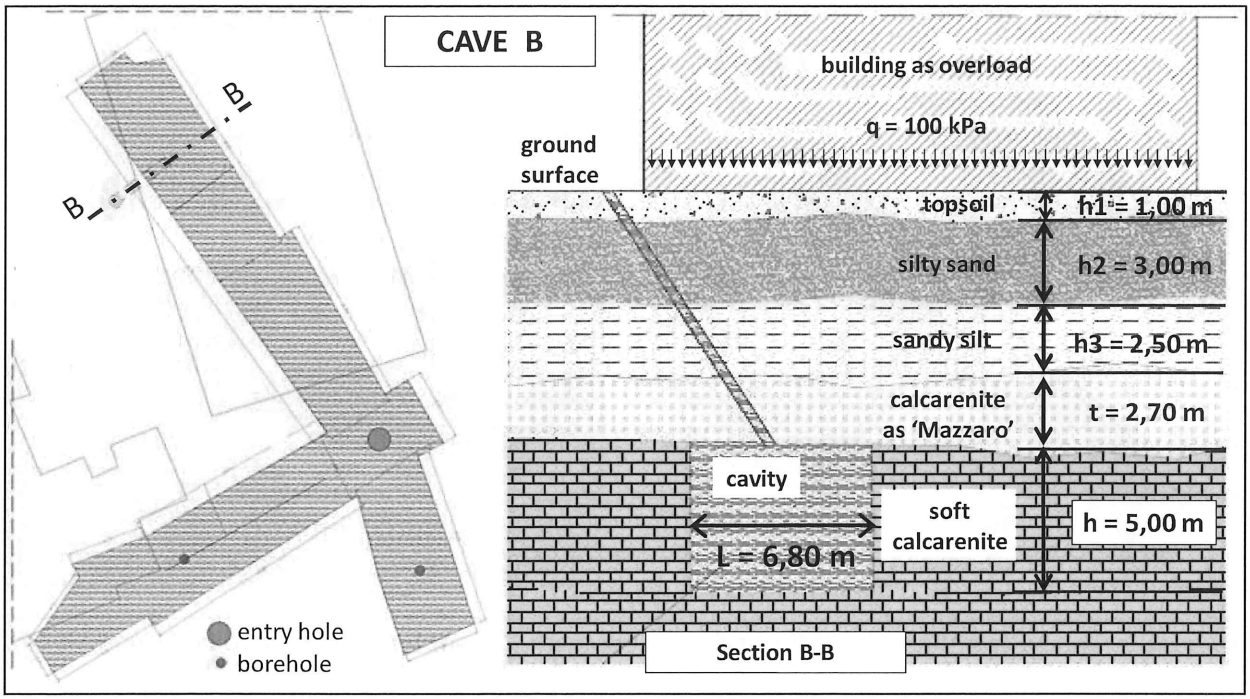

Figure 20. Plan and stratigraphy of the underground cavity B (adapted from Maglio and Ligori, 2014).

With reference to the stratigraphy in Figure 16, the vertical stress at the depth of the cavity roof is equal to:

$$\sigma_v \approx (\gamma_1 \cdot t_1) + (\gamma_2 \cdot t_2) + (\gamma_3 \cdot t_3) + (\gamma_4 \cdot t_4) + (\gamma_{mazzaro} \cdot t_{mazzaro}) + q = 277.89 \text{ kPa}$$

So that, if $\sigma_c = 2.4$ MPa, the mobilized value of σ_c/σ_v is equal to 8.64.

3.4.3. Cave C

For cave C the calculation has been performed for section C-C in Figure 21. The cave width and height are, respectively, equal to L = 5.50 m and h = 7.00 m, while the thickness of the resistant roof is t = 5.00 m and the corresponding non-dimensional ratios result about L/t ≈ 1.1 and L/h ≈ 0.79.

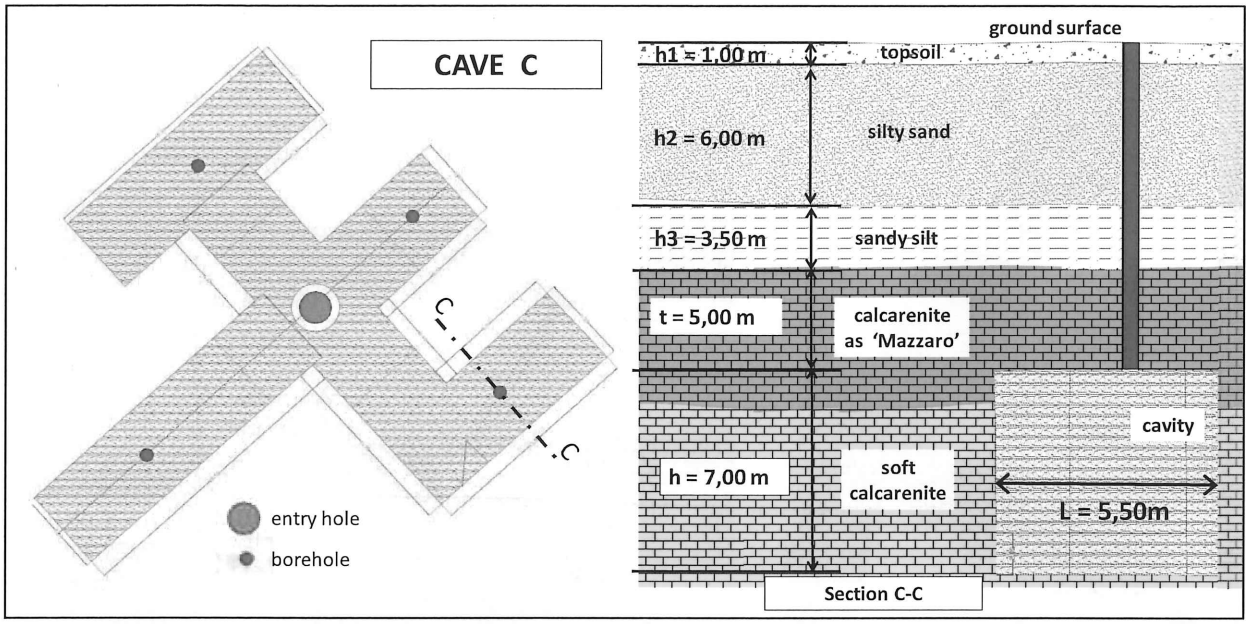

Figure 21. Plan and stratigraphy of the underground cavity C (adapted from Maglio and Ligori, 2014).

In this case, the vertical stress at the depth of the cavity roof results to be:

$\sigma_v \approx (\gamma_1 \cdot t_1) + (\gamma_2 \cdot t_2) + (\gamma_3 \cdot t_3) + (\gamma_4 \cdot t_4) + (\gamma_{mazzaro} \cdot t_{mazzaro}) = 299.7$ kPa

and assuming $\sigma_c = 2.4$ MPa, we obtain $\sigma_c/\sigma_v \approx 8$.

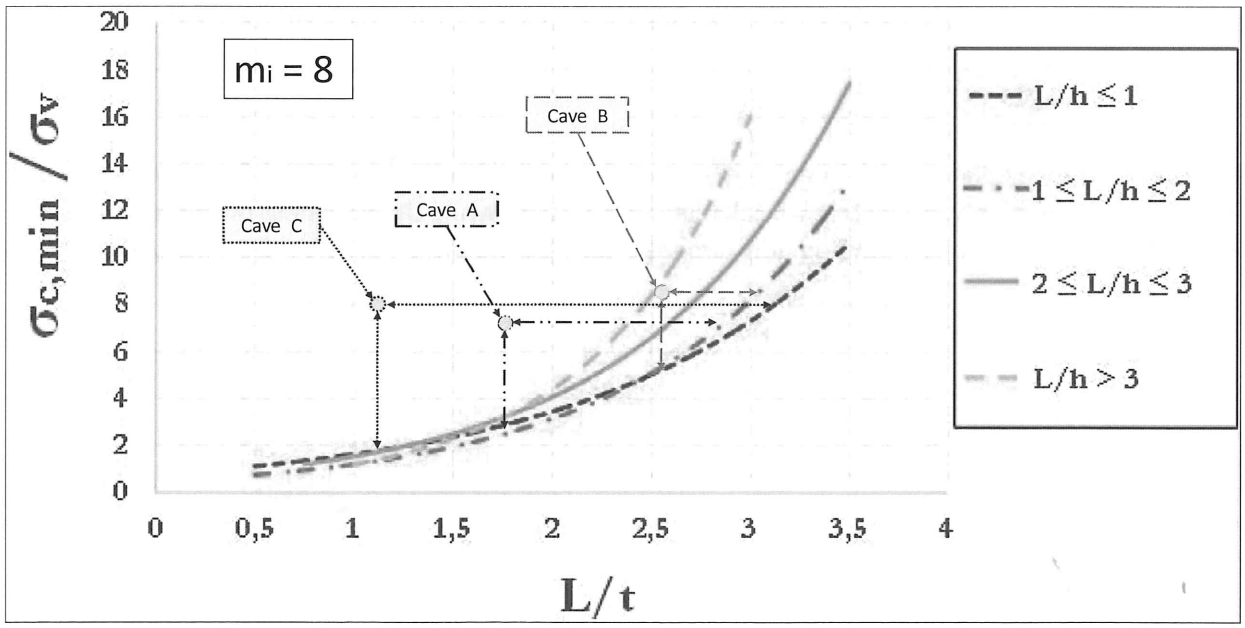

Figure 22. Application of the stability chart ($m_i = 8$) to the three underground quarries at Cutrofiano.

480 It can be pointed out that all the three cavities are in the stable zone of the chart of Figure 22,
481 although with different safety margins; in fact, the margin of safety for Cave B is low, even for the
482 presence of the overlying building. Cave A and cave C seem to be the most stable, also in relation to
483 the geometry of the caves as well as to the thickness of the "Mazzaro" resistant layer.
484
485
486
487
488 **4. Discussion and concluding remarks**
489

What is the inovation of the paper related to this previous paper?

490 In this paper, six case studies of underground artificial cavities, including three affected by sinkhole
491 failures in the past and three in stable conditions at present, have been presented, aimed at
492 application of the stability charts proposed by Perrotti et al. (2018). The proposed stability charts
493 have been verified to represent a valid method to assess the stability of underground cavities in soft
494 carbonate rocks. The study of sinkholes is generally very complex, due to both the problem of
495 reconstructing the geometric scheme before failure, and to the difficulties in identifying the
496 corresponding triggering factors. Moreover, these types of failure occur for abandoned cavities for
497 which a detailed geometry is typically not available (the Marsala case, here presented, was an
498 exception to this rule). Nevertheless, post-failure in situ surveys can help in this task and bring out,
499 especially, what are the most likely causes leading to collapse.

500 For the Barletta and Marsala sinkhole case studies, the failure of the underground cave highlighted
501 the vulnerability of the internal supporting elements, as singular pillars, on the entire system of
502 quarry: as such, the loss of material strength with time, due to weathering effects, could lead to
503 local instabilities, as detachments of rocks from the pillars, and, consequently, a reduction of the
504 resistant cross-section that, in the long term, could result in a general pillar crushing. If the
505 surrounding pillars are not able to sustain the stresses redistributed due to the previous instabilities,
506 a progressive failure process of the internal pillars is likely to occur. This, in turn, leads to the increase
507 of the distance between supporting elements, i.e. the cavity width, and therefore the possible
508 general failure of the whole cave, with development of a proper sinkhole (generally, of the collapse
509 or cover collapse types; see Gutierrez et al. 2014). Similarly, as well as the pillars, even the partition
510 walls can also represent weakness elements of the system, especially when they are thin. Typically,
511 soft and very soft rocks are exposed at a natural process of degradation (mainly due to the
512 weathering effects with cyclical and seasonal fluctuations of water content) that may accelerate
513 when overloads induced by underground works or vehicular traffic are applied. In an incipient state
514 of collapse, such as that found in the stability chart of the Gallipoli underground quarry, low rates
515 of vibrations could lead toward an acceleration of crack tensile opening with, consequently,
516 propagation of fractures and formation of a sinkhole.

the first crater?

The main assumptions are...?

517 When underground quarries are suitably surveyed and mapped, a quantitative assessment of the
518 stability conditions is possible; from this point of view, as shown for the three cases of underground
519 quarries at Cutrofiano, stability charts allow preliminarily to evaluate the risk of an incipient
520 collapse. For all the Cutrofiano case studies, stability charts have been applied for the section where
521 the ratio L/t is the biggest within the cavity, in order to consider the most dangerous area in terms
522 of safety: they resulted in stable conditions, even though with different safety margins.
523 Furthermore, using stability charts is possible, within the same cavity, to distinguish the areas more

susceptible to instability phenomena. Based on these evaluations, the management of underground quarries may change according to the evolution of the corresponding stability conditions.

How do you update the model?

It is important to highlight once again that the use of stability charts is limited to the stage of preliminary analysis. This means that such charts, especially when built upon a very high number of cases, could be extremely useful to technicians and practitioners for a first evaluation of the stability conditions. However, in case a proneness to collapse is ascertained through the stability chart, it is absolutely necessary to move to the next stage, by carrying out site-specific tests and geotechnical laboratory tests on rock samples for the determination of the parameters needed for a full analysis of stability. The main limit of such an approach is therefore represented by an erroneous use of the charts, with the wrong belief that they could act as substitute to in situ and laboratory tests. Notwithstanding such drawback, the approach here presented can definitely be of help, especially when a high number of cavities need to be initially assessed, as concerns the stability standpoint.

Please write it in the abstract

References

Andriani, G.F., Walsh, N. Petrophysical and mechanical properties of soft and porous building rocks used in apulian monuments (South Italy). Geol. Soc., London, Spec. Publ., 333, 129–141, 2010.

Cai, M. Practical estimates of tensile strength and Hoek–Brown strength parameter mi of brittle rocks. Rock Mech. Rock Eng., 43(2), 167–184, 2010.

Carter, T.G. Guidelines for use of the scaled span method for surface crown pillar stability assessment Ontario Ministry of Northern Development and Mines, 2010, pp. 1–34, 2014.

Castellanza, R., Lollino, P., Ciantia, M.O. A methodological approach to assess the hazard of underground cavities subjected to environmental weathering. Tunnelling and Underground Space Technology 82:278-292. Elsevier. DOI: 10.1016/j.tust.2018.08.041, 2018.

Ciantia, M.O., Castellanza, R., Di Prisco, C. Experimental study on the water-induced weakening of calcarenites. Rock Mech. Rock Eng., 48(2), 441–461, 2015.

Coviello, A., Lagioia, R., Nova, R. On the measurement of the tensile strength of soft rocks. Rock Mech. Rock Eng., 38(4), 251–273, 2005.

De Giovanni, A., Martimucci, V., Marzulli, M., Parise, M., Pentimone, N., Sportelli, D. Operazioni di rilievo e analisi preliminare dello sprofondamento in località San Procopio (Barletta) del 2-3 maggio 2010. Opera Ipogea, Journal of Speleology in Artificial Cavities, 1-2, pp. 151-158, 2011.

Delle Rose, M. La voragine di Gallipoli e le attività di protezione civile dell'IRPI-CNR. Geologi e Territorio. n° 4-2006 / 1-2007 pp. 3-12, 2007.

566 Evangelista, A., Pellegrino, A., Viggiani, C. Cavità e gallerie nel Tufo Giallo Napoletano. Atti IX Ciclo
567 Conf. MIR, Le opera in sotterraneo e il rapporto con l'ambiente, Patron Editore. FALLA
568 CASTELFRANCHI M. (1991) Pittura monumentale bizantina in Puglia. Milan, Italy, 2003.
569
570 Fazio, N. L., Perrotti, M., Lollino, P., Parise, M., Vattano, M., Madonia, G., Di Maggio, C. A three-
571 dimensional back-analysis of the collapse of an underground cavity in soft rocks. Engineering
572 Geology, 228, 301-311, 2017.
573
574 Federico, F., Screpanti, S. Effects of filling shallow room and pillar mines in weak pyroclastic rock.
575 Proc., XIII European Conference on Soil Mechanics and Geotechnical Engineering, Geotechnical
576 Problems with Man-made and Man Influenced. Grounds, Prague, The
577 Czech Republic, 2003.
578
579 Ferrero, A. M., Segalini, A., Giani, G. P. Stability analysis of historic underground quarries. Comput.
580 Geotech., 37(4), 476–486, 2010.
581
582 Fiore, A., Fazio, N. L., Lollino, P., Luisi, M., Miccoli, M. N., Pagliarulo, R., Perrotti, M., Pisano, L.,
583 Spalluto, L., Vennari, C., Vessia G., Parise, M. Evaluating the susceptibility to anthropogenic
584 sinkholes in Apulian calcarenites, southern Italy. Geological Society, London, Special
585 Publications, 466, 381-396, https://doi.org/10.1144/SP466.20, 2018.

586 Fiore, A., Parise, M. Cronologia degli eventi di sprofondamento in Puglia, con particolare
587 riferimento alle interazioni con l'ambiente antropizzato. Memorie Descrittive della Carta Geologica
588 d'Italia, 93, 239-252, 2013.
589
590 Fraldi, M., Guarracino, F. Limit analysis of collapse mechanisms in cavities and tunnels according to
591 the Hoek–Brown failure criterion. Int. J. Rock Mech. Min. Sci., 46(4), 665–673, 2009.
592
593 Gesualdo, A., Minutolo, V., and Nunziante, L. Failure in Mohr–Coulomb soil cavities. Can. Geotech.
594 J., 38(6), 1314–1320, 2001.
595
596 Goodings, D. J., Abdulla, W. A. Stability charts for predicting sinkholes in weakly cemented sand
597 over karst limestone. Eng. Geol., 65(2–3), 179–184, 2002.
598
599 Gutierrez, F., Parise, M., De Waele, L., Jourde, H. A review on natural and human-induced
600 geohazards and impacts in karst. Earth Science Reviews, 138, 61-88, 2014.
601
602 Hoek, E. Strength of rock and rock masses. News J. ISRM, 2(2), 4–16, 1994.
603
604 Hoek E. Practical rock engineering.
605 (https://www.rocscience.com/documents/hoek/corner/Practical-Rock-Engineering-Full-Text
606 .pdf), 2007.
607
608 Hoek, E., Brown, E. T. Practical estimates of rock mass strength. Int. J. Rock Mech. Min. Sci., 34(8),
609 1165–1186, 1997.
610
611 Hoek, E., Martin, C. D. Fracture initiation and propagation in intact rock–A review. J. Rock Mech.
612 Geotech. Eng., 6(4), 287–300, 2014.

Lollino, P., Parise, M. Analisi numerica di processi di instabilità di cavità sotterranee e degli effetti indotti in superficie. Proc. 2nd Int. Workshop "I sinkholes. Gli sprofondamenti catastrofici nell'ambiente naturale ed in quello antropizzato", Rome, 3-4 December 2009, 803.816, 2010.

Luisi, M., Di Santo, A., Fiore, A., Lepore, D., Lollino, P., Miccoli, M.N., Parise, M., Spalluto, L. Modellazione numerica 3D agli elementi finiti (FEM) per la valutazione delle condizioni di stabilità di cavità antropiche del territorio pugliese: il caso studio della cava ipogea di San Procopio (Barletta, Murge settentrionali). Mem. Descr. Carta Geol. d'It. XCIX, 327 – 336, 2015.

Maglio, A., Ligori, F. Intervento di bonifica e messa in sicurezza di cavità antropiche presenti nell'area urbana e suburbana. Studio di prefattibilità ambientale Maggio 2014. Comune di Cutrofiano. Ministero dell'Ambiente della Tutela del Territorio e del Mare, 2014.

Parise, M. The impacts of quarrying in the Apulian karst. In: Carrasco, F., La Moreaux, J.W., Duran Valsero, J.J., Andreo, B. (eds.), Advances in research in karst media. Springer, p. 441-447, 2010.

Parise, M. A present risk from past activities: sinkhole occurrence above underground quarries. Carbonates and Evaporites, 27 (2), 109-118, 2012.

Parise, M., Lollino, P. A preliminary analysis of failure mechanisms in karst and man-made underground caves in Southern Italy. Geomorphology, 134(1–2), 132–143, 2011.

Parise, M., De Giovanni, A., Martimucci, V. Sinkholes caused by underground quarries: the case of the 2–3 May 2010, event at Barletta (Southern Italy). Speleology and Spelestology, Proceedings IV International Scientific Conference, November 2013, Nabereznye Chelny (Russia), 158-162, 2013.

Perrotti, M., Lollino, P., Fazio, N.L., Pisano, L., Vessia, G., Parise, M., Fiore, A., Luisi, M. Finite element-based stability charts for underground cavities in soft calcarenites, International Journal of Geomechanics, 10.1061/(ASCE)GM.1943-5622.0001175, 2018.

Suchowerska, A. M., Merifield, R. S., Carter, J. P., Clausen, J. "Prediction of underground cavity roof collapse using the Hoek–Brown failure criterion." Comput. Geotech., 44, 93–103, 2012.

Vattano, M., Di Maggio, C., Madonia, G., Parise, M., Lollino, P., Bonamini, M. Examples of anthropogenic sinkholes in Sicily and comparison with similar phenomena in southern Italy. In: Proc. 13th Multidisc. Conf., May 6–10, Carlsbad, New Mexico. NCKRI Symposium, vol. 2. pp. 263–271, 2013.